

# Supporting Information

Umezawa et al. 10.1073/pnas.0907095106

## SI Methods

**Experimental Conditions for NanoLC-MS/MS Analysis.** Digestion of immunoprecipitated SnRK2-GFP. SRK2E- or SRK2I-GFP were prepared by immunoprecipitation from *Arabidopsis* cultured cells as described in the Methods. The affinity resin was suspended with 100  $\mu$ L of 0.1 M Tris-HCl (pH 9.0) containing 8 M urea, phosphatase inhibitor mixture 1 and 2 (Sigma-Aldrich), and phosphatase inhibitor mixture (Sigma). The suspension was reduced with DTT, alkylated with iodoacetamide, and digested with Lys-C, followed by dilution and trypsin digestion, as described previously (1). These digested samples were desalted using StageTips with C18 Empore disk membranes (3M) (2).

**Enrichment of phosphopeptides with metal oxide chromatography.** Metal oxide chromatography (MOC) using titania was performed as described in the literature (3), with slight modifications. Custom-made MOC tips were prepared using C8-StageTips and metal oxide bulk beads (0.5 mg beads per 10- $\mu$ L pipette tip), as described for SCX(beads)-C18 tips (4). Before loading samples, the MOC tips were equilibrated with 0.1% TFA and 80% acetonitrile with 300 mg/mL lactic acid as selectivity enhancers (solution A). The digested sample was diluted with 100  $\mu$ L solution A and loaded to the MOC tip. After successive washing with solution A and solution B (0.1% TFA and 80% acetonitrile), 0.5% piperidine was used for elution (5). The eluted fraction was acidified with TFA, desalted using C18 StageTips as described above, and concentrated in a vacuum evaporator, followed by addition of solution A for subsequent nanoLC-MS/MS analysis.

**NanoLC-MS/MS system.** NanoLC-MS/MS analyses were conducted using LTQ-Orbitrap (Thermo Fisher Scientific), a Dionex Ultimate3000 pump with a FLM-3000 flow manager, and an HTC-PAL autosampler. ReproSil C18 material (3  $\mu$ m, Dr. Maisch, Ammerbuch, Germany) was packed into a self-pulled needle (150-mm length  $\times$  100- $\mu$ m I.D., 6- $\mu$ m opening) with a nitrogen-pressurized column loader cell (Nikkyo Technos) to prepare an analytical column needle with “stone-arch” frit (6). A PTFE-coated column holder (Nikkyo) was mounted on an x-y-z nanospray interface (Nikkyo), and a Valco metal connector with a magnet was used to hold the column needle and to set the appropriate spray position. The injection volume was 5  $\mu$ L and the flow rate was 500 nL/min. The mobile phases consisted of (A) 0.5% acetic acid and (B) 0.5% acetic acid and 80% acetonitrile.

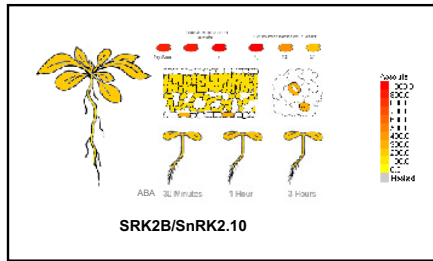
A three-step linear gradient of 5–10% B in 5 min, 10–40% B in 60 min, 40–100% B in 5 min, and 100% B for 10 min was used throughout this study. A spray voltage of 2,400 V was applied via the metal connector as described (6). The MS scan range was  $m/z$  300–1,500, and the top 10 precursor ions were selected for subsequent MS/MS scans. A lock-mass function was used for the LTQ-Orbitrap to obtain constant mass accuracy during gradient analysis (7).

**Database searching.** Mass Navigator v1.2 (Mitsui Knowledge Industry) was used to create peak lists based on the recorded fragmentation spectra as described previously (8). Peptides and proteins were identified by means of automated database searching using Mascot v2.2.04 (Matrix Science) against TAIR version 8 (02-Apr-2008), with a precursor mass tolerance of 3 ppm, a fragment ion mass tolerance of 0.8 Da, and strict trypsin specificity (9) allowing for up to two missed cleavages. Carbamidomethylation of cysteine was set as a fixed modification, and the oxidation of methionines and the phosphorylation of serine, threonine, and tyrosine were allowed as variable modifications. Peptides were considered identified if the Mascot score was above the 95% confidence limit based on the ‘identity’ score of each peptide and at least three successive y- or b-ions with an additional two and more y-, b-, and/or precursor-origin neutral loss ions were observed. All spectra were further verified by manual inspection. Note that phosphorylation can be discriminated from sulfation by LTQ-Orbitrap with the lock mass function because the error distribution is within 2 ppm (7), which is less than the mass difference between sulfation and phosphorylation (9.516 mDa) for most detectable peptides. Phosphorylated sites were determined according to localization PTM probability values based on PTM scores (10).

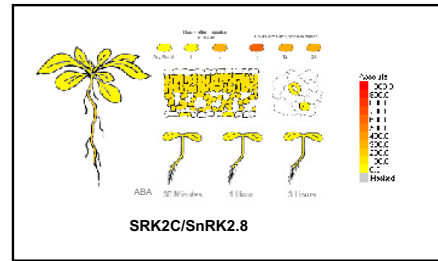
**Quantitative Analysis Using a Label-Free Approach.** The quantitative analyses of phosphorylated peptides derived from SRK2E and 2I were carried out using a label-free approach (11, 12). Peak area values in extracted ion current chromatograms were calculated using a ‘non-label quantitation’ function of Mass Navigator v1.2 with 0.005  $m/z$  range. For relative quantitation of phosphorylated peptides, the ratio of peak area ratios of a target phosphorylated peptides between samples was calculated after normalization using unmodified peptides as an internal standards (13).

1. Saito H, Oda Y, Sato T, Kuromitsu J, Ishihama Y (2006) Multiplexed two-dimensional liquid chromatography for MALDI and nano-electrospray ionization mass spectrometry in proteomics. *J Proteome Res* 5:1803–1807.
2. Rappsilber J, Ishihama Y, Mann M (2003) Stop and go extraction tips for matrix-assisted laser desorption/ionization, nano-electrospray, and LC/MS sample pretreatment in proteomics. *Anal Chem* 75:663–670.
3. Sugiyama N, et al. (2007) Phosphopeptide enrichment by aliphatic hydroxy acid-modified metal oxide chromatography for nano-LC-MS/MS in proteomics applications. *Mol Cell Proteomics* 6:1103–1109.
4. Ishihama Y, Rappsilber J, Mann M (2006) Modular stop and go extraction tips with stacked disks for parallel and multidimensional Peptide fractionation in proteomics. *J Proteome Res* 5:988–994.
5. Kyono Y, Sugiyama N, Imami K, Tomita M, Ishihama Y (2008) Successive and selective release of phosphorylated peptides captured by hydroxy acid-modified metal oxide chromatography. *J Proteome Res* 7:4585–4593.
6. Ishihama Y, Rappsilber J, Andersen JS, Mann M (2002) Microcolumns with self-assembled particle frits for proteomics. *J Chromatogr A* 979:233–239.
7. Olsen JV, et al. (2005) Parts per million mass accuracy on an orbitrap mass spectrometer via lock mass injection into a C-trap. *Mol Cell Proteomics* 4:2010–2021.
8. Ravichandran A, Sugiyama N, Tomita M, Swarup S, Ishihama Y (2009) Ser/Thr/Tyr phosphoproteome analysis of pathogenic and non-pathogenic *Pseudomonas* species. *Proteomics* 9:1–12.
9. Olsen JV, Ong S, Mann M (2004) Trypsin cleaves exclusively C-terminal to arginine and lysine residues. *Mol Cell Proteomics* 3:608–614.
10. Olsen JV, et al. (2006) Global, in vivo, and site-specific phosphorylation dynamics in signaling networks. *Cell* 127:635–648.
11. Chelius D, Bondarenko PV (2002) Quantitative profiling of proteins in complex mixtures using liquid chromatography and mass spectrometry. *J Proteome Res* 1:317–323.
12. Wang G, Wu WW, Zeng W, Chou C, Shen R (2006) Label-free protein quantification using LC-coupled ion trap or FT mass spectrometry: Reproducibility, linearity, and application with complex proteomes. *J Proteome Res* 5:1214–1223.
13. Ruse CI, et al. (2002) Quantitative dynamics of site-specific protein phosphorylation determined using liquid chromatography electrospray ionization mass spectrometry. *Anal Chem* 74:1658–1664.

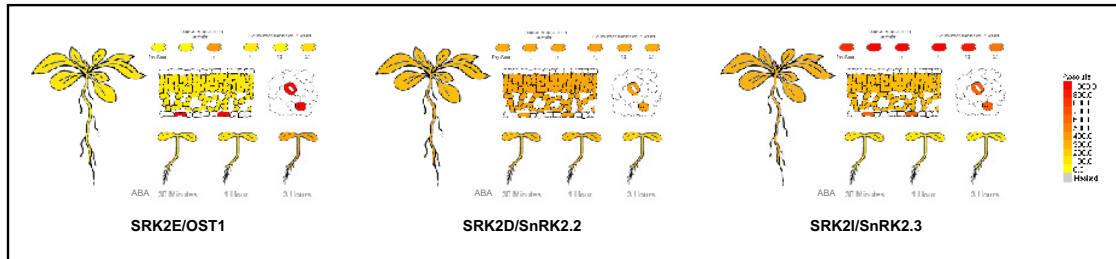
## Subclass I SnRK2



## Subclass II SnRK2



## Subclass III SnRK2



## Group A PP2C

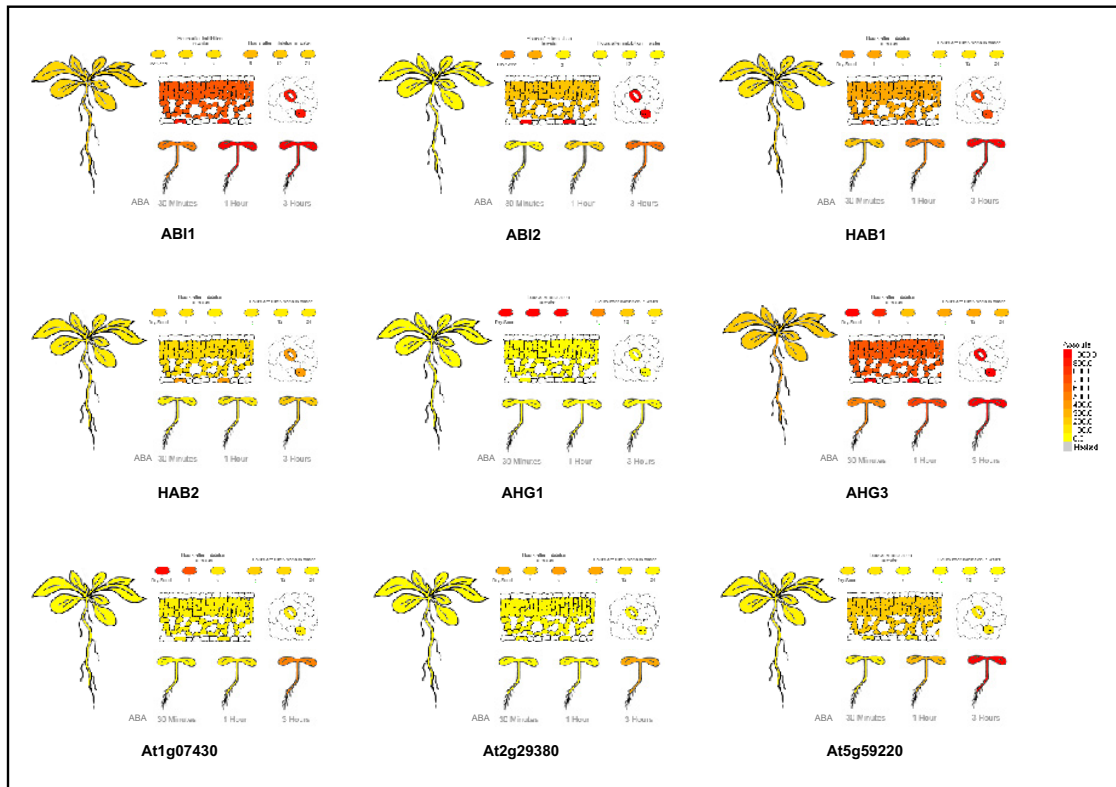


**Fig. S1.** Gene expression patterns of SnRK2s and PP2Cs. The expression data for SnRK2s and PP2Cs were collected from a public database, eFP browser (<http://bbc.botany.utoronto.ca/efp/cgi-bin/efpWeb.cgi>). This figure displays a part of the data from 'hormone,' 'tissue specific,' and 'abiotic stress' categories. Five SnRK2s and nine PP2Cs were shown: SRK2B/SnRK2.10 (At1g60940), SRK2C/SnRK2.8 (At1g78290), SRK2E/OST1/SnRK2.6 (At4g33950), SRK2D/SnRK2.2 (At3g50500), SRK2I/SnRK2.3 (At5g66880), ABI1 (At4g26080), ABI2 (At5g57050), HAB1 (At1g72770), HAB2 (At1g17550), AHG1 (At5g51760), AHG3 (At3g11410), At1g07430, At2g29380, and At5g59220. The signal threshold was manually adjusted to 1,000.



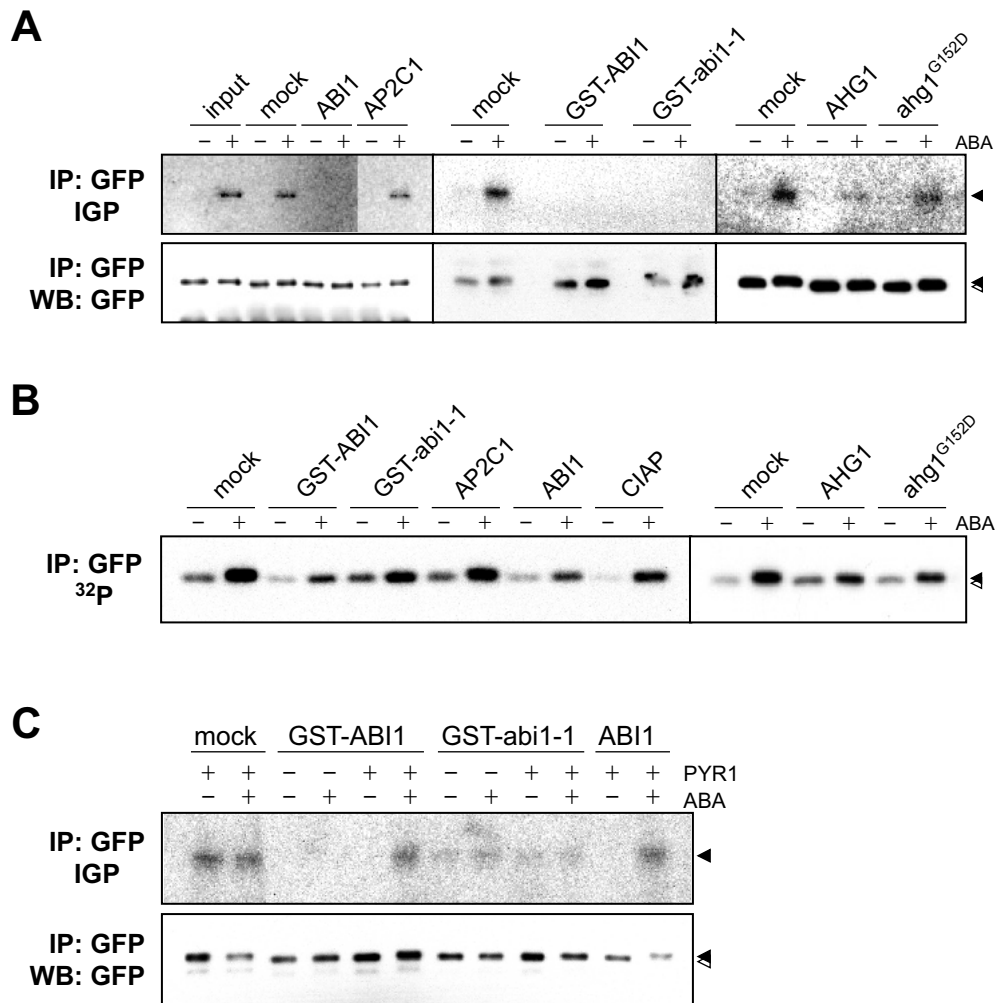
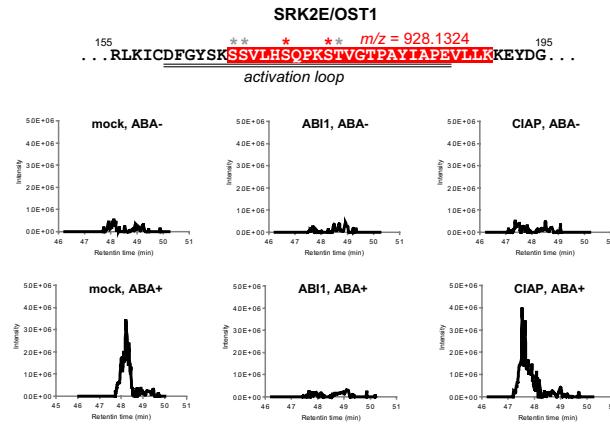


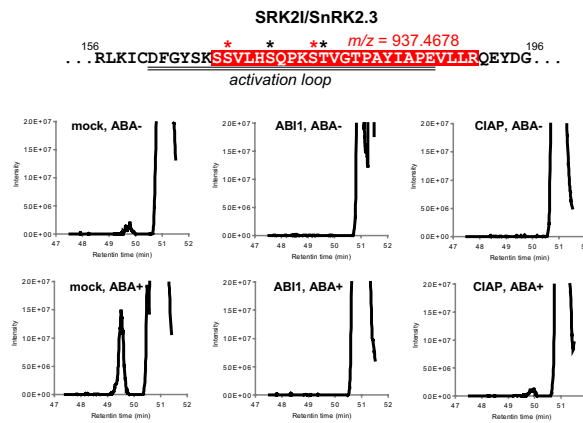
**Fig. S3.** Group A PP2Cs inactivate SRK21/SnRK2.3 via dephosphorylation. (A) In vitro reaction of SRK21-GFP and PP2Cs. GFP-tagged SRK21 proteins were collected by immunoprecipitation (IP) against an anti-GFP antibody from *Arabidopsis* cells cultured with or without ABA treatment. Bacterial recombinant PP2C proteins, ABI1, AHG1, AHG1<sup>G152D</sup>, AP2C1, GST-ABI1, and GST-abi1-1, were incubated with SRK21-GFP, and SnRK2 activity was monitored via an in-gel phosphorylation assay (IGP) using histone as a substrate. Immunoprecipitates were analyzed via Western blotting (WB) using an anti-GFP antibody. The arrows indicate SRK21-GFP. (B) In vivo Dephosphorylation levels of <sup>32</sup>P-labeled SRK21-GFP by PP2Cs. Immunoprecipitated SRK21-GFP was prepared from untreated or ABA-treated cultured cells labeled with <sup>32</sup>P-phosphate, and incubated with PP2Cs as indicated. The phosphorylation level of SRK21-GFP was monitored by SDS/PAGE and autoradiography. (C) In vitro reconstitution assay for PYR1, ABI1/abi1-1, and SRK21. Immunoprecipitated SRK21-GFP (ABA-activated) was incubated with GST-ABI1, GST-abi1-1, ABI1, or PYR1 in the presence or absence of ABA. SnRK2 activity was monitored via an in-gel phosphorylation assay (IGP) using histone as a substrate. Immunoprecipitates (IP) were checked by Western blotting (WB) against an anti-GFP antibody. Arrows indicate SRK21-GFP.



A



B



C

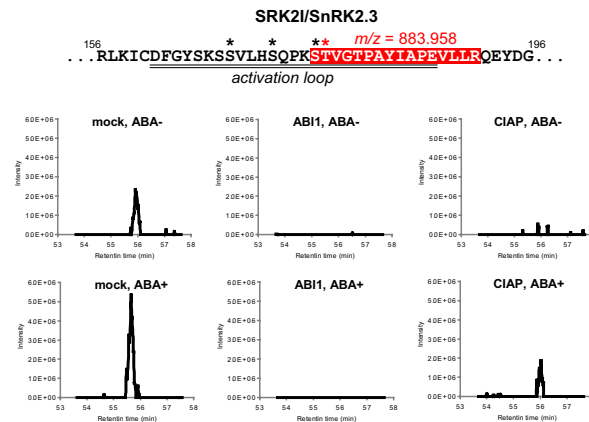


**Fig. S5.** Relative quantitation of SnRK2s-derived phosphopeptides based on the extracted ion current (XIC) chromatograms derived from nanoLC-MS/MS. SRK2E-GFP or SRK2I-GFP proteins were prepared from *Arabidopsis* cells treated with 50  $\mu$ M ABA. Immunoprecipitated SnRK2-GFP was incubated with ABI1 or CIAP and analyzed by nanoLC-MS/MS with LTQ-Orbitrap after the HAMMOC phosphopeptide enrichment. Detected phospho- or nonphospho-peptides are listed in Table S1. Mapping information and XIC chromatograms for phospho-peptides of  $m/z = 928.1324$  from SRK2E (A),  $m/z = 937.4678$  from SRK2I (B), and  $m/z = 883.958$  from SRK2I (C) are shown. Phosphorylated sites were not unambiguously identifiable in all peptides. Phosphorylated sites identified with the top PTM probability scores and other possible sites are represented by red and black asterisks, respectively. Note that no phosphorylated site met the acceptance criteria for unambiguous site determination according to PTM scores.





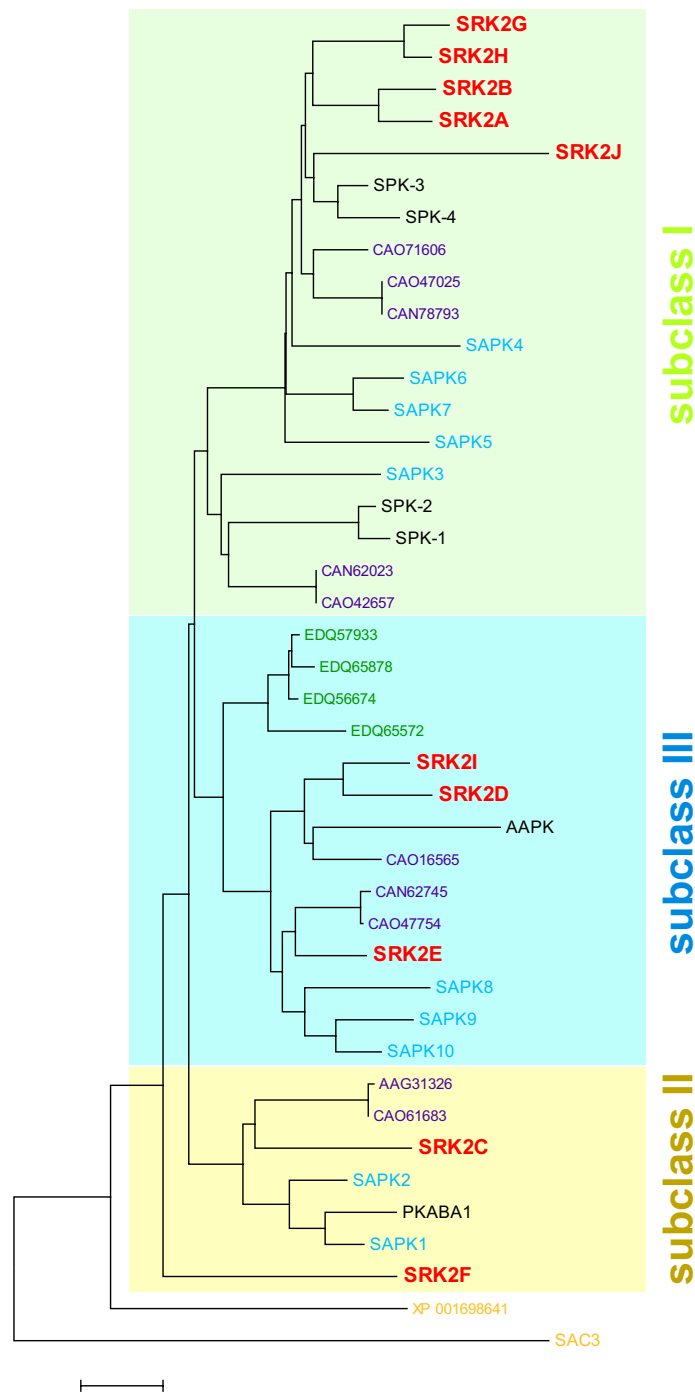


**Fig. S7.** Phylogenetic tree of SnRK2s in plants. Amino acid sequences of SnRK2 were collected from the NCBI database. We performed a BLAST search for the SRK2E sequence against the gene sets for *Arabidopsis thaliana* (red), *Oryza sativa* (blue), *Vitis vinifera* (purple), *Physcomitrella patens* (green), and *Chlamydomonas reinhardtii* (orange), and sequences containing an acidic patch (characteristic of SnRK2) with an e value  $< 1e^{-90}$  were picked up. Several other sequences, including PKABA1 from wheat, AAPK from fava bean, or SPK1–4 from soybean, were added. The phylogenetic tree was drawn using the neighbor-joining method with the MEGA 4.0 program.

## Other Supporting Information Files

[Table S1](#)